

Baryon-baryon interactions at short distances – constituent quark model meet lattice QCD –

Aaron Park,¹ Su Houng Lee,¹ Takashi Inoue,^{2,3} and Tetsuo Hatsuda^{4,3}

¹*Department of Physics and Institute of Physics and Applied Physics, Yonsei University, Seoul 03722, Korea*

²*Nihon University, College of Bioresource Sciences, Kanagawa 252-0880, Japan*

³*Quantum Hadron Physics Laboratory, RIKEN Nishina Center, Wako 351-0198, Japan*

⁴*Interdisciplinary Theoretical and Mathematical Sciences Program (iTHEMS), RIKEN, Wako 351-0198, Japan*

The interaction energies between two baryons at short distance in different flavor channels are calculated from the constituent quark model (CQM) and are compared with the recent lattice QCD (LQCD) results for baryon-baryon potentials at short distance. We consider the six-quark system with two strange quarks and focus on the quantum numbers, (Flavor, Spin)=(1,0), (8,1), (10,1), ($\overline{10}$,1) and (27,0). The interaction energy is defined by subtracting out isolated baryon masses and relative kinetic energy of two baryons from the total energy of a compact six-quark state. We introduce interaction energy ratio between different flavors as a useful measure to test the prediction of CQM. We find that the ratios in CQM show good agreement with those in LQCD, which indicates that the short range part of the baryon-baryon interaction can be understood qualitatively in terms of the Pauli principle and spin-dependent color interaction among constituent quarks.

I. INTRODUCTION

Understanding the baryon-baryon (BB) interactions at short distances is not only important to search for possible dibaryon states but also to study the central core of neutron stars. The recent analyses of the flavor dependence of the BB interactions from first principle lattice QCD (LQCD) simulations near the physical quark masses indicate that their behavior at short distances (reviewed in [1]) are qualitatively consistent with the idea of the constituent quark model (CQM) where the Pauli exclusion among quarks combined with the single gluon exchange play important roles (reviewed in [2]). However, the quantitative comparison between the LQCD results and CQM results has not been conducted so far. In this paper, we carry out such a comparison by focusing our attention on the “ratios” instead of the absolute magnitudes of the BB potentials at short distances: We expect that the interpolating operator dependence in LQCD as well as quark wave function dependence in CQM are cancelled separately in each case, so that the comparison can be made with less ambiguities in the ratio. As we will see, the color-spin-flavor structure together with the spin-dependent color interaction between quark pairs in the six-quark states provides insights into the origin of the repulsion or attraction in different flavor configurations.

This paper is organized as follows. In Sec.II, we recapitulate the essential features of the CQM which was employed to study multi-quark systems by two of the present authors [3, 4]. In Sec.III, we introduce appropriate coordinate systems to describe six-quark system containing two strange quarks. In Sec.IV, we evaluate the color-spin interactions in CQM for six-quark systems with flavor SU(3) symmetric case and compare the results with the corresponding LQCD data for heavy quark masses. In Sec. V, we evaluate the interaction energies between two baryons at short distance in CQM with flavor SU(3) non-symmetric case and compare the results

with the corresponding LQCD data for nearly physical quark masses. Sec. VI is devoted to summary and concluding remarks.

II. COMPACT SIX QUARKS IN CQM

Let us consider a compact six-quark configuration from the CQM point of view. We will assume that the spatial wave function of all the six quarks are in the lowest energy s-wave state. Because the quarks have color, flavor and spin, only specific total quantum numbers are allowed for the six quark configurations made of two octet baryons. Under flavor SU(3) symmetry, the allowed states are $(F, S) = (1, 0), (27, 0), (10, 1), (\overline{10}, 1), (8, 1)$, where F and S are the irreducible flavor representation and the total spin, respectively. In the following, we will focus on the particular isospin states with two strange quarks,

$$F_\ell \equiv (F, I, S) \\ = (1, 0, 0), (27, 0, 0), (10, 1, 1), (\overline{10}, 1, 1), (8, 0, 1), \quad (1)$$

which are relevant for making a direct comparison between the CQM results and the recent LQCD results [5]. Hereafter, we label the states in Eq.(1) by $\ell = 1, 27, 10, \overline{10}, 8$.

The interaction of two baryons at short distances in CQM [2] are governed by the quark dynamics with the following Hamiltonian,

$$H = \sum_{i=1}^N (m_i + \frac{\mathbf{p}_i^2}{2m_i}) - \frac{3}{16} \sum_{i<j}^N (V_{ij}^C + V_{ij}^{CS}), \quad (2)$$

where N is the total number of constituent quarks and m_i 's are the constituent quark masses. The spin-independent (spin-dependent) color interaction denoted as V_{ij}^C (V_{ij}^{CS}) is given by [6, 7].

$$V_{ij}^C = -\lambda_i^c \lambda_j^c \left(-\frac{\kappa}{r_{ij}} + \frac{r_{ij}}{a_0} - D \right), \quad (3)$$

κ	κ'	a_0	D	α	β	$m_{u,d}$	m_s	m_c	m_b
0.59	0.5	5.386	0.96	2.1	0.552	0.343	0.632	1.93	5.3
		GeV ⁻²	GeV	fm ⁻¹		GeV	GeV	GeV	GeV

TABLE I. The parameters of CQM fitted to light and heavy baryon masses [6].

(I, S)	$(\frac{1}{2}, \frac{1}{2})$	$(\frac{1}{2}, \frac{3}{2})$	$(0, \frac{1}{2})$	$(1, \frac{1}{2})$	$(1, \frac{3}{2})$	$(\frac{1}{2}, \frac{1}{2})$	$(\frac{1}{2}, \frac{3}{2})$
	N, P	Δ	Λ	Σ	Σ^*	Ξ	Ξ^*
M_B	0.977	1.23	1.12	1.2	1.38	1.324	1.52
Expt.	0.938	1.232	1.115	1.189	1.382	1.315	1.532

TABLE II. Masses of light baryons relevant to the present work in the unit of GeV.

$$V_{ij}^{CS} = \frac{\kappa'}{m_i m_j r_{0ij}^2} \frac{1}{r_{ij}} e^{-(r_{ij}/r_{0ij})^2} \lambda_i^c \lambda_j^c \sigma_i \cdot \sigma_j, \quad (4)$$

where λ_i^c are the Gell-Mann matrices of the i 'th quark for the color SU(3). Here, r_{ij} is the distance between quarks, while r_{0ij} is chosen to depend on the constituent quark masses as

$$r_{0ij} = (\alpha + \beta \mu_{ij})^{-1}. \quad (5)$$

with $\mu_{ij} = m_i m_j / (m_i + m_j)$ being the reduced mass.¹ Throughout this paper, we assume isospin symmetry, $m_u = m_d$. In Table I, we show the values of the parameters fitted to low-lying baryon masses with $S=1/2$ and $3/2$ including those with charm and bottom quarks [6]. Table II shows the calculated masses of light baryons relevant to this work.

The static interaction energy V_{CQM} between two baryons located on top of each other can be estimated by looking at the interaction in terms of the six-quark configuration relative to the two-baryon threshold:

$$V_{\text{CQM}} = \langle H \rangle_{6q} - E_{BB'}, \quad (6)$$

$$E_{BB'} = M_B + M_{B'} + K_{\text{rel}, BB'}. \quad (7)$$

Here $\langle H \rangle_{6q}$ is the expectation value of the Hamiltonian with $N = 6$ with respect to the six-quark in the s-wave, M_B and $M_{B'}$ are the single baryon energies obtained by the Hamiltonian with $N = 3$, and $K_{\text{rel}, BB'}$ is the relative kinetic energy between two baryons. This formula will be used to estimate the interaction energies for both the flavor SU(3) symmetric and non-symmetric cases.

¹ The quark mass dependence in r_{0ij} is introduced to fit the hadrons masses not only with light flavors but also with charm and bottom in the s-wave [6].

	$i, j=1-4$	$i=1-4, j=5,6$	$i, j=5,6$
F_1	$-\frac{7}{6}$	$-\frac{11}{12}$	$-\frac{5}{3}$
F_{27}	$-\frac{5}{6}$	$-\frac{17}{12}$	$\frac{1}{3}$
F_{10}	$-\frac{35}{27}$	$-\frac{13}{18}$	$-\frac{22}{9}$
$F_{\overline{10}}$	$-\frac{31}{27}$	$-\frac{17}{18}$	$-\frac{14}{9}$
F_8	$-\frac{4}{3}$	$-\frac{2}{3}$	$-\frac{8}{3}$

TABLE III. Expectation value of the spin-independent color factor $\langle \lambda_i^c \lambda_j^c \rangle$ of a quark pair in each flavor state. $i = 1 - 4$ label the light quarks and $i = 5, 6$ the strange quarks.

The total energy of the six-quark system in CQM can also be decomposed as

$$\langle H \rangle_{6q} = \sum_{i=1}^6 m_i + K + E_C + E_{CS}, \quad (8)$$

where K stands for the total kinetic energy, E_C is obtained from V_C and E_{CS} is obtained from V_{CS} .

The average matrix elements for the quark pairs contributing to the spin-independent color interaction V_C are given in Table III. For flavor SU(3) symmetric case with $m_s = m_u$, this interaction will not contribute in appreciable strength in Eq.(6) as long as the spatial size of a single baryon and that of the 6-quark system similar. This is so because the color factor in V_C taken with respect to the color-singlet state is proportional to N as

$$\sum_{i < j} \lambda_i^c \lambda_j^c = -\frac{8}{3}N. \quad (9)$$

This is also true for f -type or d -type three-quark interactions in the color singlet state [4]: $\sum_{i \neq j \neq k} f^{abc} \lambda_i^a \lambda_j^b \lambda_k^c = 0$ and $\sum_{i \neq j \neq k} d^{abc} \lambda_i^a \lambda_j^b \lambda_k^c = \frac{160}{9}N$ where f and d are the antisymmetric and symmetric structure constants for color SU(3), respectively.

On the other hand, the sum of the color-spin factor in the color-spin interaction V_{CS} depends non-linearly on N as will be shown in Sec.IV, so that it induces non-vanishing contribution to Eq.(6).

III. COORDINATE SYSTEM FOR SIX QUARKS

In the following, we consider V_{CQM} for the six-quark system with two strange quarks as mentioned. To calculate $\langle H \rangle_{6q}$ in Eq. (8) for different flavor states, we first construct the orbital-color-flavor-spin wave function for six-quark systems [8]. Since we place two strange quarks on the fifth and sixth positions, the total wave function of the compact six quarks should obey the $\{1234\}\{56\}$ symmetry where the curly bracket means antisymmetric combination. We choose the spatial part of the wave

function $|R\rangle$ satisfying [1234][56] with the square bracket being symmetric combination,

$$|R\rangle = \frac{1}{\sqrt{\mathcal{N}}} e^{-a_1(\mathbf{x}_1^2 + \mathbf{x}_2^2 + \mathbf{x}_3^2) - a_4\mathbf{x}_4^2 - a_5\mathbf{x}_5^2}. \quad (10)$$

Here \mathcal{N} is a normalization factor and $\mathbf{x}_1, \dots, \mathbf{x}_5$ are the Jacobi coordinates,

$$\begin{aligned} \mathbf{x}_1 &= \frac{1}{\sqrt{2}}(\mathbf{r}_1 - \mathbf{r}_2), & \mathbf{x}_2 &= \frac{1}{\sqrt{6}}(\mathbf{r}_1 + \mathbf{r}_2 - 2\mathbf{r}_3) \\ \mathbf{x}_3 &= \frac{1}{\sqrt{12}}(\mathbf{r}_1 + \mathbf{r}_2 + \mathbf{r}_3 - 3\mathbf{r}_4), & \mathbf{x}_4 &= \frac{1}{\sqrt{2}}(\mathbf{r}_5 - \mathbf{r}_6) \\ \mathbf{x}_5 &= \sqrt{\frac{4}{3}}(\mathbf{r}_{1234} - \mathbf{r}_{56}), \end{aligned} \quad (11)$$

with $\mathbf{r}_{1234} = (\mathbf{r}_1 + \mathbf{r}_2 + \mathbf{r}_3 + \mathbf{r}_4)/4$ and $\mathbf{r}_{56} = (\mathbf{r}_5 + \mathbf{r}_6)/2$. Then the color-flavor-spin part of the wave function should obey $\{1234\}\{56\}$ symmetry in order to satisfy the Pauli exclusion principle.

We introduce two additional Jacobi coordinates for the two-baryon configuration such as (qqq)+(qss) and (qqs)+(qqs) to extract the relative kinetic energy. Specifically, for the final state involving (qqq)+(qss), we transform the coordinates in Eq.(11) to the following baryon-baryon coordinates: $\mathbf{y}_1 = \frac{1}{\sqrt{2}}(\mathbf{r}_1 - \mathbf{r}_2)$, $\mathbf{y}_2 = \frac{1}{\sqrt{6}}(\mathbf{r}_1 + \mathbf{r}_2 - 2\mathbf{r}_3)$, $\mathbf{y}_3 = \frac{1}{\sqrt{2}}(\mathbf{r}_5 - \mathbf{r}_6)$, $\mathbf{y}_4 = \frac{1}{\sqrt{6}}(\mathbf{r}_5 + \mathbf{r}_6 - 2\mathbf{r}_4)$, $\mathbf{y}_5 = \sqrt{\frac{3}{2}}(\mathbf{r}_{123} - \mathbf{r}_{456})$, where $\mathbf{r}_{123} = (\mathbf{r}_1 + \mathbf{r}_2 + \mathbf{r}_3)/3$, $\mathbf{r}_{456} = (m_u\mathbf{r}_4 + m_s\mathbf{r}_5 + m_s\mathbf{r}_6)/(m_u + 2m_s)$. Similarly, for the final state involving (qqs)+(qqs), we transform the coordinates in Eq.(11) to the following baryon-baryon coordinates: $\mathbf{z}_1 = \frac{1}{\sqrt{2}}(\mathbf{r}_1 - \mathbf{r}_5)$, $\mathbf{z}_2 = \sqrt{\frac{2}{3}}(\mathbf{r}_{15} - \mathbf{r}_2)$, $\mathbf{z}_3 = \frac{1}{\sqrt{2}}(\mathbf{r}_3 - \mathbf{r}_4)$, $\mathbf{z}_4 = \frac{1}{\sqrt{6}}(\mathbf{r}_3 + \mathbf{r}_4 - 2\mathbf{r}_6)$, $\mathbf{z}_5 = \sqrt{\frac{3}{2}}(\mathbf{r}_{125} - \mathbf{r}_{346})$ where $\mathbf{r}_{15} = (m_u\mathbf{r}_1 + m_s\mathbf{r}_5)/(m_u + m_s)$, $\mathbf{r}_{125} = (m_u\mathbf{r}_1 + m_u\mathbf{r}_2 + m_s\mathbf{r}_5)/(2m_u + m_s)$, and $\mathbf{r}_{346} = (m_u\mathbf{r}_3 + m_u\mathbf{r}_4 + m_s\mathbf{r}_6)/(2m_u + m_s)$. We use these coordinates also when we evaluate the two-body interaction between the u quark and the s quark. Then the relative kinetic energies in terms of these two coordinate systems for (qqq)+(qss) or (qqs)+(qqs) are

$$K_{\text{rel}} = \frac{1}{2\mu_1} P_{\mathbf{y}_5}^2 \quad \text{or} \quad K_{\text{rel}} = \frac{1}{2\mu_2} P_{\mathbf{z}_5}^2 \quad (12)$$

with $\mu_1 = \frac{m_u(m_u + 2m_s)}{2m_u + m_s}$ and $\mu_2 = \frac{2m_u + m_s}{3}$. Note that $P_{\mathbf{y}_5}$ and $P_{\mathbf{z}_5}$ are the conjugate momenta of \mathbf{y}_5 and \mathbf{z}_5 , respectively.

IV. INTERACTION RATIOS FOR FLAVOR SU(3) SYMMETRIC CASE

Let us now consider the flavor SU(3) symmetric case where the matrix element shown below is a basic quantity

F_ℓ	F_1	F_{27}	F_{10}	$F_{\bar{10}}$	F_8
$\mathcal{R}_\ell^{\text{CQM}}$	-0.33	1	0.78	0.78	0.28
$\mathcal{R}_\ell^{\text{LQCD}}$	-0.53(3)	1	0.93(1)	0.81(1)	0.20(1)

TABLE IV. Comparison of ratios of the color-spin interactions at short distance R_ℓ between the constituent quark model (CQM) and the lattice QCD data (LQCD) in the flavor SU(3) symmetric case [9].

to determine V_{CQM} :

$$\begin{aligned} \mathcal{X} &\equiv - \sum_{i < j}^N \langle \lambda_i^c \lambda_j^c \sigma_i \cdot \sigma_j \rangle \\ &= N(N-10) + \frac{4}{3}S(S+1) + 4C_f + 2C_c. \end{aligned} \quad (13)$$

Here C_f and C_c are the first kind of Casimir operators of flavor and color for the N -quark system, respectively [10].² Assuming that the size of the quark wave-function of the six-quark system and that for each 3-quark system are the same for simplicity, we obtain, with a common constant γ ,

$$V_{\text{CQM}}(F_\ell) = \gamma(\mathcal{X}_{6q} - (\mathcal{X}_B + \mathcal{X}_{B'})). \quad (14)$$

In the following, we consider the ratios between $V_{\text{CQM}}(F_\ell)$ to get rid of the constant γ in the flavor SU(3) symmetric limit:

$$\mathcal{R}_\ell^{\text{CQM}} = \frac{V_{\text{CQM}}(F_\ell)}{V_{\text{CQM}}(F_{27})}. \quad (15)$$

Similarly, the ratios for baryon-baryon potential at $r = 0$ can be introduced as

$$\mathcal{R}_\ell^{\text{LQCD}} = \frac{V_{\text{LQCD}}(F_\ell)}{V_{\text{LQCD}}(F_{27})}. \quad (16)$$

As mentioned in the Introduction, the quark wave function dependence in CQM and the interpolating operator dependence in LQCD are expected to cancel independently in such ratios, so that the comparison can be made with less ambiguities.

In Table IV, we compare $\mathcal{R}_\ell^{\text{CQM}}$ from the color-spin interaction in the flavor SU(3) case and $\mathcal{R}_\ell^{\text{LQCD}}$ obtained from the currently available lattice data in the flavor SU(3) case [9] with the pseudo-scalar meson mass $M_{\text{ps}} \simeq 469$ MeV and the octet baryon mass $M_B \simeq 1161$ MeV. The errors in the parentheses for $\mathcal{R}_\ell^{\text{LQCD}}$ reflect the combined statistical and systematic errors estimated

² More explicitly, $C_f = \frac{1}{3}(p^2 + q^2 + 3(p+q) + pq)$ with $(p, q) = (0, 0)$ for flavor SU(3) singlet, (1,0) for triplet, (1,1) for octet, (2,2) for 27-plet, (3,0) for decuplet, and (0,3) for anti-decuplet. The same holds for C_c in color SU(3). For the simplest case with $N = 1$, we have $(p, q) = (1, 0)$ in both color and flavor, so that $C_f = C_c = 4/3$.

from the LQCD data at the Euclidean time $t = 11$ and 12. One finds that the sign and magnitude of these ratios are qualitatively consistent with each other between CQM and LQCD.

V. INTERACTION RATIOS FOR FLAVOR SU(3) NON-SYMMETRIC CASE

Let us now examine the flavor SU(3) non-symmetric case where the color-spin factor receives additional constituent quark mass dependence as follows [11],

$$\mathcal{Y}_\ell \equiv - \sum_{i < j}^6 \frac{1}{m_i m_j} \langle \lambda_i^c \lambda_j^c \sigma_i \cdot \sigma_j \rangle_{F_\ell}. \quad (17)$$

Their explicit forms read

$$\begin{aligned} \mathcal{Y}_1 &= -\frac{5}{m_u^2} - \frac{22}{m_u m_s} + \frac{3}{m_s^2}, \\ \mathcal{Y}_{27} &= -\frac{13}{3m_u^2} + \frac{26}{3m_u m_s} + \frac{11}{3m_s^2}, \\ \mathcal{Y}_{10} &= \frac{98}{27m_u^2} - \frac{100}{27m_u m_s} + \frac{74}{27m_s^2}, \\ \mathcal{Y}_{\overline{10}} &= \frac{106}{27m_u^2} - \frac{116}{27m_u m_s} + \frac{82}{27m_s^2}, \\ \mathcal{Y}_8 &= -\frac{16}{3m_u^2} - \frac{20}{3m_u m_s} + \frac{8}{3m_s^2}. \end{aligned} \quad (18)$$

The numerical coefficients in Eq. (18) are obtained by combining the color-spin factor for an (i, j) -pair, $-\lambda_i^c \lambda_j^c \sigma_i \cdot \sigma_j$, with the probability of finding an (i, j) -pair in the six-quark state, $P_{ij}(F_\ell)$, given in Table V. For example, the color-spin factor -5 in front of $1/m_u^2$ for \mathcal{Y}_1 in Eq. (18) is obtained by using the four factors for $i, j=1-4$ in the 6th and 7th rows of Table V as follows,

$$\left(\frac{1}{4} \cdot (-8) + \frac{1}{4} \cdot \left(-\frac{4}{3}\right) + \frac{3}{8} \cdot \frac{8}{3} + \frac{1}{8} \cdot 4 \right) \cdot \binom{4}{2} = -5, \quad (19)$$

where $\binom{4}{2}$ is the number of light quark pairs inside the six-quark system. Other coefficients can be obtained similarly by further noting that the number of light-strange (strange-strange) quark pairs is 8 (1). The explicit form of $P_{ij}(F_\ell)$ is given by

$$P_{ij}(F_\ell) = \langle \Psi_{F_\ell} | \hat{\mathcal{P}}_{ij} | \Psi_{F_\ell} \rangle, \quad (20)$$

with a projection operator, $\hat{\mathcal{P}}_{ij} \equiv |\psi_{ij}^d\rangle \langle \psi_{ij}^d| \otimes \mathbf{1}$, where ψ_{ij}^d is the wavefunction of the relevant diquark that satisfies a certain symmetry property represented in Table V, while $\mathbf{1}$ is a unit operator acting on the particles other than i and j .

There are a few points to be noted. First, the isospin determines whether the color-spin factors coming from

	$i, j = 1-4$				$i = 1-4, j = 5, 6$				$i, j = 5, 6$	
ψ_{ij}^d	A				M				A	
color	A	S	A	S	A	S	A	S	A	S
flavor	A	A	S	S	M				S	S
spin	A	S	S	A	A	S	S	A	S	A
$-\lambda_i^c \lambda_j^c \sigma_i \cdot \sigma_j$	-8	$-\frac{4}{3}$	$\frac{8}{3}$	4	-8	$-\frac{4}{3}$	$\frac{8}{3}$	4	$\frac{8}{3}$	4
$P_{ij}(F_1)$	$\frac{1}{4}$	$\frac{1}{4}$	$\frac{3}{8}$	$\frac{1}{8}$	$\frac{3}{8}$	$\frac{3}{8}$	$\frac{3}{16}$	$\frac{1}{16}$	$\frac{3}{4}$	$\frac{1}{4}$
$P_{ij}(F_{27})$	$\frac{1}{4}$	$\frac{1}{4}$	$\frac{7}{24}$	$\frac{5}{24}$	$\frac{1}{8}$	$\frac{1}{8}$	$\frac{9}{16}$	$\frac{3}{16}$	$\frac{1}{4}$	$\frac{3}{4}$
$P_{ij}(F_{10})$	$\frac{5}{36}$	$\frac{7}{36}$	$\frac{14}{27}$	$\frac{4}{27}$	$\frac{5}{24}$	$\frac{7}{24}$	$\frac{11}{36}$	$\frac{7}{36}$	$\frac{17}{18}$	$\frac{1}{18}$
$P_{ij}(F_{\overline{10}})$	$\frac{5}{36}$	$\frac{7}{36}$	$\frac{13}{27}$	$\frac{5}{27}$	$\frac{5}{24}$	$\frac{7}{24}$	$\frac{13}{36}$	$\frac{5}{36}$	$\frac{3}{18}$	$\frac{5}{18}$
$P_{ij}(F_8)$	$\frac{1}{4}$	$\frac{1}{4}$	$\frac{5}{12}$	$\frac{1}{12}$	$\frac{7}{32}$	$\frac{11}{32}$	$\frac{9}{32}$	$\frac{5}{32}$	1	0

TABLE V. Color-spin factor and the probability P_{ij} for (i, j) diquark pairs with S, A and M representing symmetric (S), antisymmetric (AS) and mixed (M) combinations.

the two light quarks, shown in the first terms in Eq. (18), are attractive ($I=0$) or repulsive ($I=1$). As can be seen from the P 's appearing in the second and third columns of Table V, all the $I=0$ flavor states have the same contributions to the color-spin factor from the attractive light-light diquarks, which are also larger than those from the $I=1$ case. Furthermore, the large attraction in the F_1 channel as seen in the second term in the first line of Eq. (18) follows from the large additional attraction between the light-strange diquarks, which can be seen to follow from the relatively large contribution from the attractive maximally antisymmetric color-spin configuration often referred to as the ‘‘good diquark’’. Finally, as can be seen in Table V, the light-strange diquarks have mixed flavor symmetry as they do not have to satisfy Pauli principle in flavor SU(3) breaking case.

To calculate the interaction energy in each flavor channel F_ℓ , we need to subtract $E_{BB'}$ in Eq. (7) from $\langle H \rangle_{F_\ell}$ with appropriate SU(3) CG coefficients [12]:

$$\begin{aligned} V_{\text{CQM}}(F_1) &= \langle H \rangle_{F_1} - \left[\frac{1}{8} E_{\Lambda\Lambda} + \frac{3}{8} E_{\Sigma\Sigma} + \frac{1}{2} E_{N\Xi} \right], \\ V_{\text{CQM}}(F_{27}) &= \langle H \rangle_{F_{27}} - \left[\frac{27}{40} E_{\Lambda\Lambda} + \frac{1}{40} E_{\Sigma\Sigma} + \frac{3}{10} E_{N\Xi} \right], \\ V_{\text{CQM}}(F_{10}) &= \langle H \rangle_{F_{10}} - \left[\frac{1}{2} E_{\Sigma\Lambda} + \frac{1}{6} E_{\Sigma\Sigma} + \frac{1}{3} E_{N\Xi} \right], \\ V_{\text{CQM}}(F_{\overline{10}}) &= \langle H \rangle_{F_{\overline{10}}} - \left[\frac{1}{2} E_{\Sigma\Lambda} + \frac{1}{6} E_{\Sigma\Sigma} + \frac{1}{3} E_{N\Xi} \right], \\ V_{\text{CQM}}(F_8) &= \langle H \rangle_{F_8} - E_{N\Xi}. \end{aligned} \quad (21)$$

The total energy of the six quarks $\langle H \rangle_{F_\ell}$ is given by calculating each term in Eq.(8) and minimizing the sum with respect to the variational parameters a_1, a_4, a_5 in Eq.(10). Resulting total energy and its decomposition are shown in Table VI for each flavor state.

F_ℓ	$\langle H \rangle_{6q}$	K	E_C	E_{CS}	a_1	a_4	a_5
F_1	2596.2	1717.9	-1447.4	-310.3	2.17	3.11	2.72
F_{27}	2900.7	1373.6	-1142.9	34.0	1.78	1.95	2.40
F_{10}	2889.2	1372.2	-1154.7	35.7	1.74	2.86	1.85
$F_{\overline{10}}$	2900.3	1377.4	-1145.2	32.2	1.73	2.60	2.14
F_8	2735.2	1526.0	-1306.7	-120.2	2.0	3.01	1.91

TABLE VI. Energies of the six-quark states in MeV unit. K , E_C and E_{CS} represent the total kinetic energy, confinement potential energy and color-spin potential energy, respectively. a_1 , a_4 and a_5 are variational parameters in fm^{-2} unit.

Corresponding LQCD data in each flavor channel F_ℓ can be obtained by relating the results of the baryon mass eigenstates to that of six-quark flavor eigenstates [13] with the same SU(3) CG coefficients as those in Eq.(21). By using LQCD data for two baryons at nearly physical quark masses corresponding to $(M_\pi, M_K, M_N, M_\Lambda, M_\Sigma, M_\Xi) \simeq (146, 525, 956, 1121, 1201, 1328)$ MeV, the diagonal parts of the potentials in the flavor-space $V_{\text{LQCD}}(F_\ell)$ have been obtained in [5].

In Table VII, we compare the ratios $\mathcal{R}_\ell^{\text{LQCD}}$ obtained in this way and $\mathcal{R}_\ell^{\text{CQM}}$ obtained from Eq.(15) using Eq.(21). The errors in the parentheses for $\mathcal{R}_\ell^{\text{LQCD}}$ reflect the combined statistical and systematic errors estimated from the LQCD data at the Euclidean time $t = 11$ and 12. Again, we find that the sign and magnitude of these ratios are qualitatively consistent between CQM and LQCD.

F_ℓ	F_1	F_{27}	F_{10}	$F_{\overline{10}}$	F_8
$\mathcal{R}_\ell^{\text{CQM}}$	-0.19	1	0.77	0.80	0.42
$\mathcal{R}_\ell^{\text{LQCD}}$	-0.43(14)	1	0.97(4)	0.82(1)	0.26(2)

TABLE VII. Comparison of the ratios of short distance interactions R_ℓ between the constituent quark model (CQM) and the lattice QCD data (LQCD) in the flavor SU(3) non-symmetric case [5].

To see how the interaction ratios in LQCD change as a function of r at short distances, we plot $\mathcal{R}_\ell^{\text{LQCD}}$ obtained at finite r (black dots and red triangles) in Figs. 1-4 together with $\mathcal{R}_\ell^{\text{CQM}}$ (black solid lines and red dashed lines) evaluated at $r = 0$. The error bars contain both statistical and systematic errors estimated from the LQCD data at $t = 11$ and 12. One finds that the interaction ratio introduced in the present paper is rather insensitive to the quark masses and flavor SU(3) breaking at short distances, $r < 0.2$ fm.

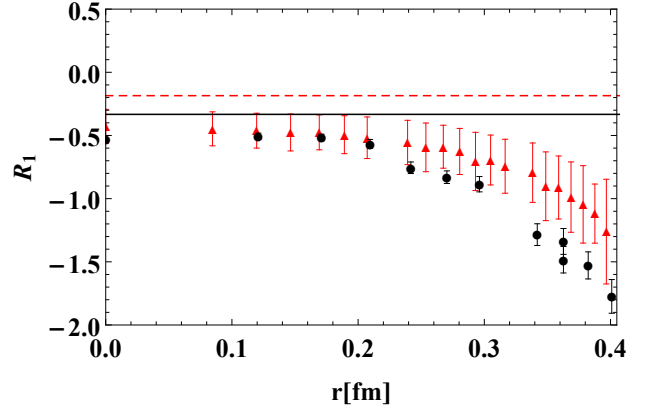


FIG. 1. The Interaction ratios $\mathcal{R}_1^{\text{LQCD}}$ evaluated for finite r are plotted by black dots (SU(3) symmetric case [9]) and red triangles (SU(3) non-symmetric case [5]). The quark model results evaluated at $r = 0$ are shown by the black solid line (SU(3) symmetric case) and the red dashed line (SU(3) non-symmetric case for comparison).

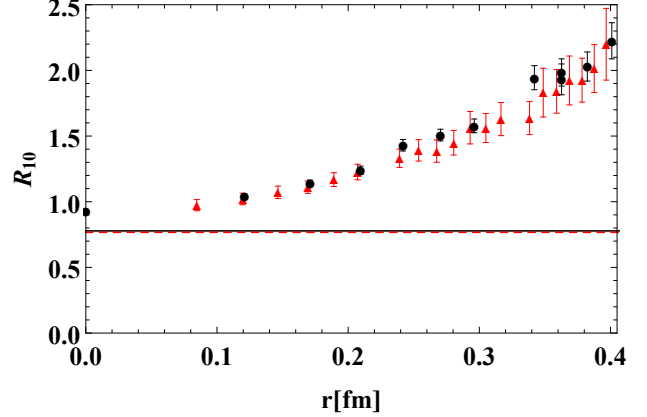


FIG. 2. Same as Fig. 1 for $\mathcal{R}_{10}^{\text{LQCD}}$.

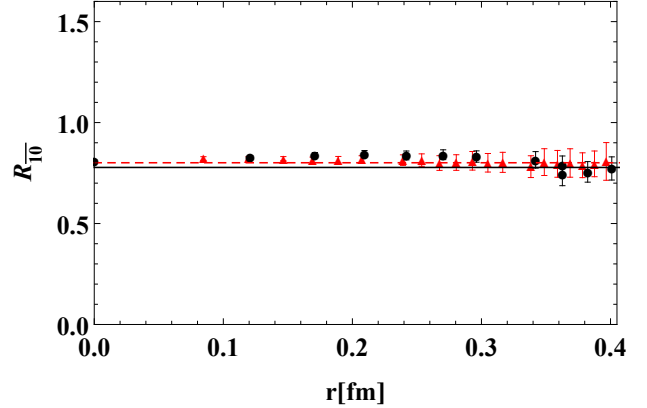


FIG. 3. Same as Fig. 1 for $\mathcal{R}_{\overline{10}}^{\text{LQCD}}$.

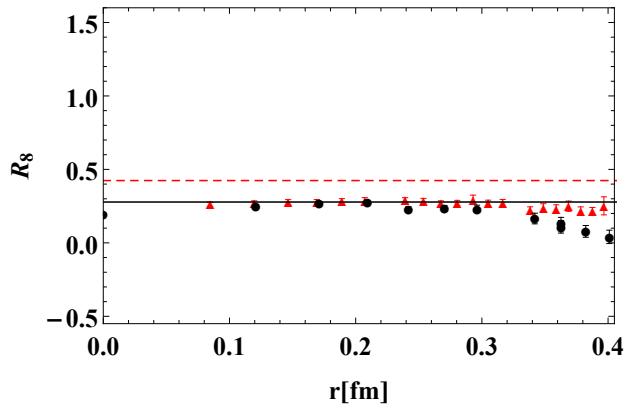


FIG. 4. Same as Fig. 1 for $\mathcal{R}_8^{\text{LQCD}}$.

VI. SUMMARY AND CONCLUDING REMARKS

Great progress has been made recently towards understanding nuclear force starting directly from QCD using lattice gauge theory. Traditionally, nuclear force is divided into short range repulsion, intermediate attraction, and long range pion exchange. In this work we have shown that the short range part of the baryon-baryon interaction in different flavor channels extracted from lattice calculation can be quantitatively understood in terms of Pauli principle and the quark-quark interaction. In channels where a compact six-quark state are Pauli blocked, the baryon interaction is highly repulsive. However, when the channels are Pauli allowed, the interaction can either be attractive or repulsive mainly depending on the sum of color-spin dynamics between quarks. In fact, the quark dynamics responsible for short range attraction between two baryons in certain channels provide a reason for the possible existence of dibaryon states (either compact or molecular type) in the same quantum numbers, such as the elusive H-dibaryon. Also, by analyzing the color-flavor-spin wave function and all possible diquark configuration contributing to a given six-quark state with two strange quarks, we have shown that the large attraction originates from the light-light diquark in the iso-singlet and spin-singlet channel as well as the light-strange diquark in the spin-singlet channel. This

implies the crucial role of "good diquarks" in the multi-quark system with strangeness.

There are still rooms for improvement in our work. For more quantitative comparison between CQM and LQCD, the contributions from non-zero quark orbital states should be taken into account. Appendix A contains useful matrix elements for such extended analysis. Furthermore, to go beyond the discussions limited to short distance we have to properly include further non-perturbative quark dynamics and/or the effects of flavor-spin dynamics through pseudo-scalar meson exchange [14]. Such issues will be discussed in the future.

ACKNOWLEDGMENTS

The work by SHL was supported by Samsung Science and Technology Foundation under Project Number SSTF-BA1901-04. This work by AP was supported by the Korea National Research Foundation under the grant number 2018R1D1A1B07043234. The work by T.H. was supported by JSPS Grant-in-Aid for Scientific Research (S), No. 18H05236. We thank H. Nemura for carefully reading the manuscript.

Appendix A: Beyond s-wave orbital for six-quark state in CQM

In the main text, we focus only on the s-wave orbitals for the 6-quark systems to extract the interaction V_{CQM} . When the two baryons overlap with each other, however, there arise four possible orbital states in general. They are characterized by the Young tableau as,

$$[3]_O \times [3]_O = [6]_O + [51]_O + [42]_O + [33]_O.$$

Flavor-spin structure associated with each orbital state for color-singlet 6-quark is shown in the first row of TABLE VIII. Then the color-spin matrix element $\chi(F_\ell)$ for $N = 6$ (defined in the first equality in Eq.(13)) can be evaluated as summarized in TABLE VIII. The column for $[6]_O \otimes [33]_{FS}$ corresponds to the matrix elements employed in the text.

-
- [1] T. Hatsuda, Front. Phys. (Beijing) **13**, 132105 (2018).
 - [2] M. Oka, K. Shimizu and K. Yazaki, Prog. Theor. Phys. Suppl. **137**, 1 (2000).

-
- [3] W. Park, A. Park and S. H. Lee, Phys. Rev. D **93**, 074007 (2016) [arXiv:1602.05017 [hep-ph]].
 - [4] A. Park, W. Park and S. H. Lee, Phys. Rev. D **98**, 034001

	$[6]_O \otimes [33]_{FS}$	$[51]_O \otimes [42]_{FS}$	$[42]_O \otimes [51]_{FS}$	$[42]_O \otimes [33]_{FS}$	$[33]_O \otimes [42]_{FS}$
$\mathcal{X}_{6q}(F_1)$	-24	p.f.	p.f.	-14	p.f.
$\mathcal{X}_{6q}(F_{27})$	8	p.f.	$\frac{16}{9}$	$-\frac{38}{9}$	p.f.
$\mathcal{X}_{6q}(F_{10})$	$\frac{8}{3}$	$\frac{16}{15}$	$-\frac{128}{9}$	$-\frac{26}{9}$	$-\frac{4}{3}$
$\mathcal{X}_{6q}(F_{\overline{10}})$	$\frac{8}{3}$	p.f.	$\frac{16}{9}$	$-\frac{26}{9}$	p.f.
$\mathcal{X}_{6q}(F_8)$	$-\frac{28}{3}$	$\frac{2}{15}(-67 \pm 3\sqrt{241})$	$-\frac{80}{9}$	$-\frac{59}{9}$	$\frac{1}{6}(-41 \pm 3\sqrt{457})$

TABLE VIII. The expectation value of color-spin interaction with respect to the 6-quark systems with mixed orbital symmetry in flavor SU(3) symmetric case. The elements with “p.f.” in the Table correspond to the Pauli forbidden states.

- (2018) [arXiv:1801.10350 [hep-ph]].
- [5] T. Inoue [HALQCD Collaboration], PoS INPC **2016**, 277 (2016) [arXiv:1612.08399 [hep-lat]].
 - [6] A. Park, W. Park and S. H. Lee, Phys. Rev. D **94**, 054027 (2016) [arXiv:1606.01006 [hep-ph]].
 - [7] R. K. Bhaduri, L. E. Cohler and Y. Nogami, Nuovo Cim. A **65**, 376 (1981). doi:10.1007/BF02827441
 - [8] W. Park, A. Park and S. H. Lee, Phys. Rev. D **92**, 014037 (2015) [arXiv:1506.01123 [nucl-th]].
 - [9] T. Inoue *et al.* [HAL QCD Collaboration], Nucl. Phys. A **881**, 28 (2012) [arXiv:1112.5926 [hep-lat]].
 - [10] A. T. M. Aerts, P. J. G. Mulders and J. J. de Swart, Phys. Rev. D **17**, 260 (1978).
 - [11] B. Silvestre-Brac and J. Leandri, Phys. Rev. D **45**, 4221 (1992).
 - [12] J. J. de Swart, Rev. Mod. Phys. **35**, 916 (1963) [Erratum: Rev. Mod. Phys. **37**, 326 (1965)].
 - [13] K. Sasaki *et al.* [HAL QCD Collaboration], PTEP **2015**, 113B01 (2015) [arXiv:1504.01717 [hep-lat]].
 - [14] L. Y. Glozman and D. O. Riska, Phys. Rept. **268**, 263 (1996) [hep-ph/9505422].